

Flt3 inhibitor AC220 is a potent therapy in a mouse model of myeloproliferative disease driven by enhanced wild-type Flt3 signaling

Samuel J. Taylor,¹ Samantha A. Dagger,¹ Christine B. F. Thien,¹ Matthew E. Wikstrom,² and Wallace Y. Langdon,¹

¹School of Pathology and Laboratory Medicine, University of Western Australia, Crawley, Australia; and ²Centre for Experimental Immunology, Lions Eye Institute, Nedlands, Australia

High levels of expression of wild-type Flt3 characterize many hematopoietic proliferative diseases and neoplasms, providing a potential therapeutic target. Using the c-Cbl RING finger mutant mouse as a model of a myeloproliferative disease (MPD) driven by wild-type Flt3, in the present study, we show that treatment with the Flt3 kinase inhibitor AC220 blocks MPD development by targeting Flt3⁺ multipotent progenitors (MPPs). We found that daily administration of AC220 caused

a marked reduction in Flt3 expression, induction of quiescence, and a significant loss of MPPs within 4 days. Unexpectedly, a robust Flt3 ligand-associated proliferative recovery response soon followed, preventing further loss of MPPs. However, continued AC220 treatment limited MPP recovery and maintained reduced, steady-state levels of cycling MPPs that express low levels of Flt3. Therefore, a finely tuned balance between the opposing forces of AC220 and Flt3

ligand production was established; whereas the Flt3 ligand blunted the inhibitory effects of AC220, the disease was held in remission for as long as therapy was continued. The net effect is a potent therapy indicating that patients with c-Cbl mutations, or those with similarly enhanced Flt3 signaling, may respond well to AC220 even after the induction of high levels of Flt3 ligand. (*Blood*. 2012;120(19):4049-4057)

Introduction

The Flt3 receptor tyrosine kinase is expressed at high levels on most myeloid and lymphoblastic leukemias,¹ and for many years it has been considered a potential target for compounds that inhibit its kinase activity.^{2,3} However, it has been difficult to test this possibility because of a lack of both suitable animal models and Flt3 inhibitors with the desired potency, specificity, and pharmacokinetic properties. Recently, we characterized a mouse with an inactivating knock-in mutation in the RING finger domain of the c-Cbl E3 ubiquitin ligase that has provided a model for studying myeloid malignancies driven by enhanced Flt3 signaling. This mouse develops a myeloproliferative disease (MPD) progressing to lethal leukemia that is characterized by markedly elevated WBC counts, splenomegaly, and extensive myeloid cell invasion into peripheral organs.⁴ Analysis of Lin⁻Sca-1⁺c-Kit⁺ (LSK) cells in the BM revealed a marked expansion of cells expressing high levels of Flt3 compared with LSK cells from wild-type and c-Cbl-deficient mice.⁴ Furthermore, the Flt3⁺ LSK cells (defined as multipotent progenitors, MPPs)⁵ showed enhanced Flt3 signaling to the Erk and PI3K pathways. When these mice were mated to Flt3 ligand-deficient mice, the doubly mutant mice did not develop leukemia,⁴ indicating that Flt3 signaling is an essential component for driving disease development.

Mutations in *c-Cbl* have been identified in 5%-20% of patients within the World Health Organization (WHO) groupings of myelodysplastic syndrome (MDS) and myelodysplastic/myeloproliferative neoplasm (MDS/MPN).⁶⁻¹⁴ MDS/MPN patients are further classified into chronic myelomonocytic leukemia, juvenile myelomonocytic leukemia, and atypical chronic myeloid leukemia. MDS

and chronic myelomonocytic leukemia are the most common blood disorders of the elderly and, because no standardized therapy has proven effective, these patients have a poor prognosis.^{15,16} Within the MDS classification, most patients with c-Cbl mutations have been identified in the subgroup of refractory anemia with excess blasts, many of whom progress to secondary acute myeloid leukemia (AML).^{7,12} Indeed, a high occurrence of c-Cbl mutations was recently found in high-risk MDS patients who progress to AML.¹⁷ c-Cbl mutations have also been identified in AML,¹⁸⁻²² the blast crisis phase of chronic myeloid leukemia,²³ infant and childhood acute lymphoblastic leukemia,²⁴⁻²⁶ and childhood therapy-related leukemia.

Sequencing of the *c-Cbl* gene has shown that the mutations are located in the linker or RING finger domains either as missense mutations or exon 8 deletions. Mutations within these domains have been extensively characterized and found to abolish c-Cbl E3 ubiquitin ligase activity by disrupting the interaction with E2 ubiquitin-conjugating enzymes.²⁷⁻²⁹

AC220 (also known as quizartinib) is the first Flt3 kinase inhibitor to show excellent potency, selectivity, and pharmacokinetic properties,³⁰ a profile highly desirable for a clinical inhibitor. Therefore, it is showing promise in clinical trials treating leukemia patients with activating Flt3 internal tandem duplication mutations.³¹ However, little is known about whether Flt3 inhibitors can be used to treat leukemias that are driven by enhanced wild-type Flt3 signaling. Using c-Cbl RING finger mutant mice, in the present study, we show that an MPD that is dependent on wild-type Flt3 signaling can be treated effectively with AC220.

Submitted June 12, 2012; accepted September 10, 2012. Prepublished online as *Blood* First Edition paper, September 18, 2012; DOI 10.1182/blood-2012-06-436675.

The online version of this article contains a data supplement.

The publication costs of this article were defrayed in part by page charge payment. Therefore, and solely to indicate this fact, this article is hereby marked "advertisement" in accordance with 18 USC section 1734.

© 2012 by The American Society of Hematology

Methods

Mice

The generation of c-Cbl(C379A) RING finger mutant mice (ie, c-Cbl^{Δ/-} mice) has been described previously.³² C57BL/6.CD45.1 congenic mice were purchased from the Animal Resource Center. All mouse experiments were approved and performed in accordance with the guidelines and regulations of the Animal Ethics Committee of the University of Western Australia (approval 100/909 and 100/786). Mice were housed under pathogen-free conditions in micro-isolator cages at the animal facilities of the University of Western Australia.

AC220 dosing

Mice were treated daily with 10 mg/kg of AC220 (quizartinib hydrochloride salt; Ambit Biosciences) or vehicle (5% 2-hydroxypropyl-β-cyclodextrin; Sigma-Aldrich) by oral gavage using 20-gauge, 1.5-inch feeding needles (Braintree). To deliver a 100-μL dose of 10 mg/kg to a 25-g mouse, AC220 was prepared at 2.5 mg/mL in 5% 2-hydroxypropyl-β-cyclodextrin. Experiments involved 2 groups of mice. The first group was C57BL/6.CD45.1 mice lethally irradiated (2 × 5.5 Gy) at 9 weeks of age and repopulated by tail vein injection with 2 × 10⁶ BM cells from 8- to 10-week-old c-Cbl^{Δ/-} mutant mice. The second group was naturally bred c-Cbl^{Δ/-} mutant mice 8-9 months of age. After the dosing ceased, most mice were killed for the analysis of BM, spleen, and peripheral organs. In some experiments, the mice were left untreated for various periods to determine whether the effects of AC220 were temporary or maintained.

Analysis of peripheral blood and BM cells

Blood was collected from the tail vein and differential cell counts determined using a Hemavet HV950FS blood analyzer (Drew Scientific). BM cells were analyzed by flow cytometry (FACSCanto; BD Biosciences) and cell sorting (Influx; BD Biosciences) using the following mAbs (all from BD Biosciences unless noted otherwise): CD3-biotin, CD11b-FITC, CD11b-PE, or CD11b-biotin, CD16/32-PE, CD19-PE, CD34-FITC, CD45.1-FITC, CD45.2-APC (eBiosciences), c-Kit-APC, Sca-1-PE-Cy7, B220-biotin, Flt3-PE (eBiosciences), Gr-1-FITC or Gr-1-biotin, IL-7R-biotin, and TER119-biotin. Cells incubated with biotinylated Abs were treated with streptavidin conjugated with APC-Cy7 (BD Biosciences). Cell-cycle analysis was performed either by examining BM cells fixed with Cytofix/Cytoperm (BD Biosciences) or Cytofix/Cytoperm reagents A and B (Invitrogen) and stained with anti-Ki-67-FITC Abs or FITC-labeled isotype control Abs (BD Biosciences) and Hoechst 33342 (Sigma-Aldrich) at 20 μg/mL. Intracellular phospho-S6 ribosomal protein (Ser235/236) was also examined using Cytofix/Cytoperm-treated cells and an Alexa Fluor 647-conjugated rabbit Ab (Cell Signaling Technology). Cell death of hematopoietic progenitors was determined using an Annexin V-FITC apoptosis detection kit (BD Biosciences) according to the manufacturer's directions. The data were collected using CellQuest Version 6 software (BD Biosciences) and analyzed using FlowJo Version 9.3.1 software (TreeStar).

ELISA

Serum levels of Flt3 ligand and SCF were determined using Quantikine immunoassay kits following the manufacturer's directions (R&D Systems).

Histopathology

Organs were fixed in Bouin fixative for 48 hours, followed by 2 sequential washes in 70% ethanol. Tissue processing was carried out using a Leica TP 1020 processor, and 5-μm sections were stained with H&E. Tissue sections were examined using an Olympus BX51 microscope and photographed with an SIS 3VCU Olympus digital camera.

Statistical analyses

To validate the significance of the observed differences between AC220 and vehicle-treated groups, we used unpaired 2-sided t tests analyzed with

Prism Version 5 software (GraphPad). *P* < .05 was considered statistically significant. All statistical data are presented as means ± SEM.

Results

AC220 markedly reduces WBC counts in c-Cbl RING finger mutant mice

Because homozygous c-Cbl RING finger mutant mice die in utero, we routinely analyzed c-Cbl(C379A) knock-in mice expressing a single mutant c-Cbl RING finger allele and a c-Cbl null allele (ie, c-Cbl^{Δ/-} mice). These mice are generated from matings between c-Cbl^{-/-} × c-Cbl^{Δ/+} mice.³²

To determine the effectiveness of AC220 for treating MPD in c-Cbl RING finger mutant mice, we established 2 cohorts, 1 comprising 18 naturally bred c-Cbl^{Δ/-} mice 8-9 months of age and another comprising 16 lethally irradiated C57BL/6.CD45.1 mice transplanted with BM from an 8-week-old c-Cbl^{Δ/-} mouse and aged for 6 months (termed here CD45.1^{Δ/-} mice). The examination of transplanted mice was to control for nonhematopoietic effects of the c-Cbl mutation, which may affect responses to AC220. The mice were dosed once daily for 6 weeks by oral gavage with 10 mg/kg of AC220 or vehicle.

Mice were bled for 5 days before dosing, and again at 3 and 6 weeks to determine numbers of WBCs, neutrophils, lymphocytes, and monocytes (Figure 1A-B). Before treatment, the assigned AC220 and vehicle groups within each cohort had equivalent WBC counts, with the naturally bred c-Cbl^{Δ/-} mice exhibiting higher counts than the CD45.1^{Δ/-} mice (pretreatment means of 61 × 10⁹/L and 34 × 10⁹/L, respectively). For comparison, c-Cbl^{+/-} littermates at 8-9 months of age have WBC counts of 10-15 × 10⁹/L.⁴

Dosing with AC220 resulted in significant (2- to 3-fold) reductions in WBC counts from both cohorts and across all major WBC types (Figure 1A-B). The effect of AC220 was clearly evident by 3 weeks and was maintained at 6 weeks. In contrast, WBC counts from the vehicle-treated groups remained high. The effectiveness of AC220 in reducing peripheral WBC counts is illustrated by representative blood films from vehicle- and AC220-treated c-Cbl^{Δ/-} mice (Figure 1C). However, the WBC counts did not decrease to wild-type levels, suggesting that the degree of inhibition was not complete or that additional factors may be involved.

Suppression of MPD is not maintained after cessation of AC220 treatment

After 6 weeks of dosing, 4 CD45.1^{Δ/-} mice and 3 c-Cbl^{Δ/-} mice were left untreated for 4 weeks to determine whether suppression of their WBC counts could be maintained after cessation of AC220 treatment. The CD45.1^{Δ/-} mice showed a decrease of WBC counts from an average of 36 × 10⁹/L to 18 × 10⁹/L after 6 weeks of AC220, and this increased to 24 × 10⁹/L 4 weeks after treatment was discontinued (Figure 2A). The effects on c-Cbl^{Δ/-} mice were even more profound, with a reduction in WBC counts from 84 × 10⁹/L to 22 × 10⁹/L after 6 weeks of AC220, and this was mostly reversed after 4 weeks without AC220, increasing to 66 × 10⁹/L (Figure 2B). These effects can be seen clearly in blood films prepared from a c-Cbl^{Δ/-} mouse at these times (Figure 2C). Therefore, suppression of c-Cbl-directed MPD requires the maintenance of AC220 treatment.

We next investigated whether mice retain their sensitivity to AC220 when exposed to a second round of dosing. CD45.1^{Δ/-} mice were dosed daily for 9 weeks with AC220 or vehicle,

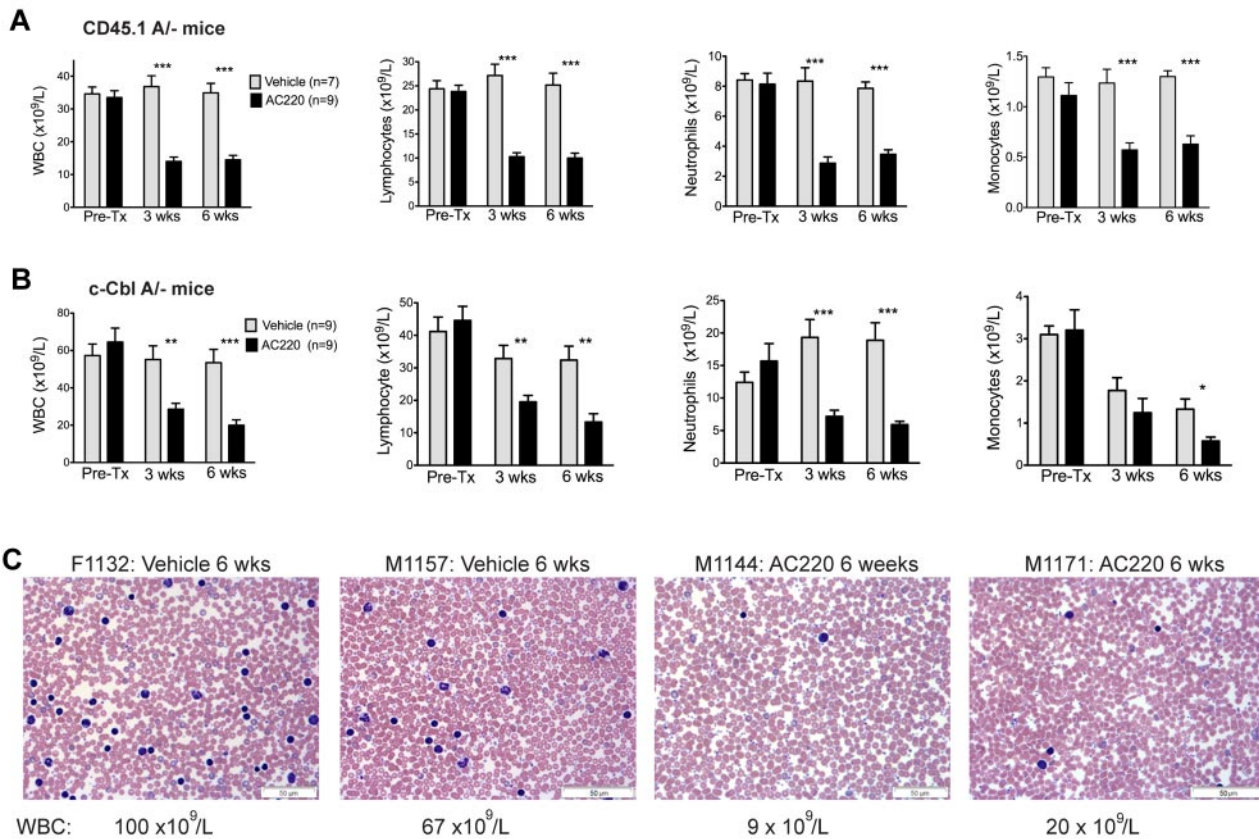


Figure 1. Treatment of c-Cbl RING finger mutant mice with AC220 results in a significant reduction in peripheral WBCs. Two cohorts of mice were examined, lethally irradiated C57BL/6.CD45.1 mice repopulated with BM cells from a c-Cbl^{Δ/Δ} mouse (CD45.1^{Δ/Δ}; A) and 8- to 9-month-old naturally bred c-Cbl^{Δ/Δ} mice (B). Both cohorts were bled for 5 days before dosing (Pre-Tx) and after 3 and 6 weeks of dosing. Results are from Hemavet analysis of blood collected from the tail vein. Shown are numbers of WBCs, lymphocytes, neutrophils, and monocytes. The blood counts are expressed as means ± SEM. Treatment of both cohorts with AC220 resulted in statistically significant decreases in WBCs, neutrophil, lymphocyte, and monocyte counts compared with the vehicle-treated mice. **P* < .05; ***P* < .01; ****P* < .001 using unpaired Student *t* test. (C) Representative blood films from 2 vehicle- and 2 AC220-treated c-Cbl^{Δ/Δ} mice after 6 weeks of dosing. The identification numbers and sex of the mice are indicated (F, female) and (M, male). The images were acquired at room temperature using an Olympus BX51 microscope with a 60×/0.09 objective and photographed with an SIS 3VCU Olympus digital camera. Scale bar indicates 50 μm.

followed by 9 weeks without dosing, before recommencing AC220 treatment for both groups for an additional 6 weeks (supplemental Figure 1, available on the *Blood* Web site; see the Supplemental Materials link at the top of the online article). Consistent with the findings shown in Figure 2, there was a return to the MPD

phenotype after the cessation of AC220 dosing. When dosing recommenced, the mice that had previously been exposed to AC220 or vehicle responded with an equivalent and marked reduction in their WBC counts. None of the mice developed resistance to the inhibitory effects of AC220. However, the

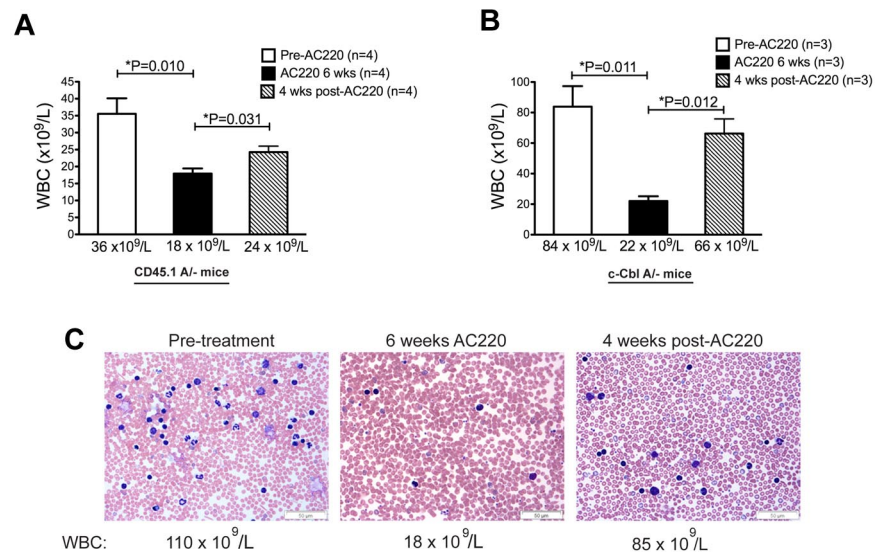


Figure 2. Myeloproliferative disease returns when AC220 treatment is discontinued. WBC counts are from 4 C57BL/6.CD45.1 mice repopulated with BM cells from a c-Cbl^{Δ/Δ} mouse (A) and three 8- to 9-month-old naturally bred c-Cbl^{Δ/Δ} mice (B). The mice were bled for 5 days before treatment commenced, after 6 weeks of daily dosing with vehicle or AC220, and 4 weeks after AC220 treatment was discontinued. (C) Blood films from a c-Cbl^{Δ/Δ} mouse (M1173) before treatment, after 6 weeks of dosing with AC220, and 4 weeks after AC220 dosing was discontinued. The images were acquired at room temperature using an Olympus BX51 microscope with a 60×/0.09 objective and photographed with an SIS 3VCU Olympus digital camera. The WBC counts are shown and the scale bar indicates 50 μm.

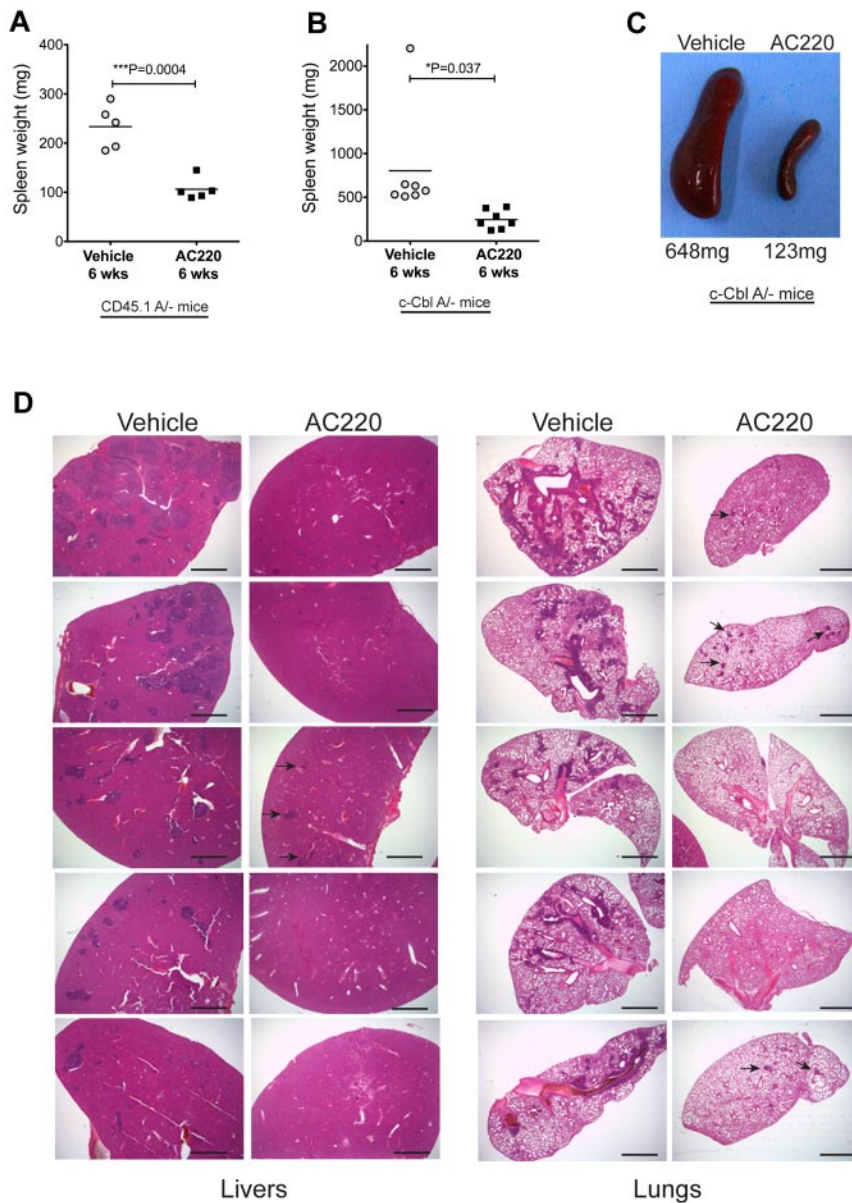


Figure 3. AC220 treatment of c-Cbl RING finger mutant mice results in a significant reduction of splenomegaly and the loss of invasive myeloid-lineage cells from the liver and lungs. Spleen weights were determined after 6 weeks of daily dosing with vehicle or AC220 of C57BL/6.CD45.1 mice repopulated with BM cells from an 8-week-old c-Cbl^{A/-} mouse (A) and 8- to 9-month-old naturally bred c-Cbl^{A/-} mice (B). (C) Photograph of spleens from a vehicle- and an AC220-treated c-Cbl^{A/-} mouse after 6 weeks of dosing. (D) H&E-stained sections of livers and lungs from c-Cbl^{A/-} mice 8-9 months of age that were dosed daily for 6 weeks with vehicle or AC220. The AC220-treated mice showed a marked reduction in myeloid cell invasion, with residual regions of infiltrating cells in AC220-treated mice indicated by arrows. The images were acquired at room temperature using an Olympus BX51 microscope with a 2×/0.08 objective and photographed with an SIS 3VCU Olympus digital camera. Scale bar indicates 2 mm.

potential of prolonged exposure to AC220 to promote resistance should not be discounted.³³

AC220 reduces splenomegaly and invasiveness of myeloid cells into the liver and lungs

AC220 treatment was also found to have a significant effect in reducing splenomegaly and myeloid cell invasion in c-Cbl RING finger mutant mice. CD45.1^{A/-} mice dosed for 6 weeks had mean spleen weights of 106 mg in the AC220-treated group compared with 243 mg in the vehicle-treated group (Figure 3A). Similarly, AC220 dosing suppressed splenomegaly in the c-Cbl^{A/-} cohort, with mean spleen weights of 803 and 245 mg for the vehicle- and AC220-treated mice, respectively (Figure 3B-C).

Our previous study found that myeloid infiltration of peripheral organs, particularly the liver and lungs, was a likely contributor to morbidity of c-Cbl RING finger mutant mice.⁴ Analysis of 5 vehicle- and 5 AC220-treated c-Cbl^{A/-} mice after 6 weeks of dosing revealed that all mice treated with AC220 showed a marked

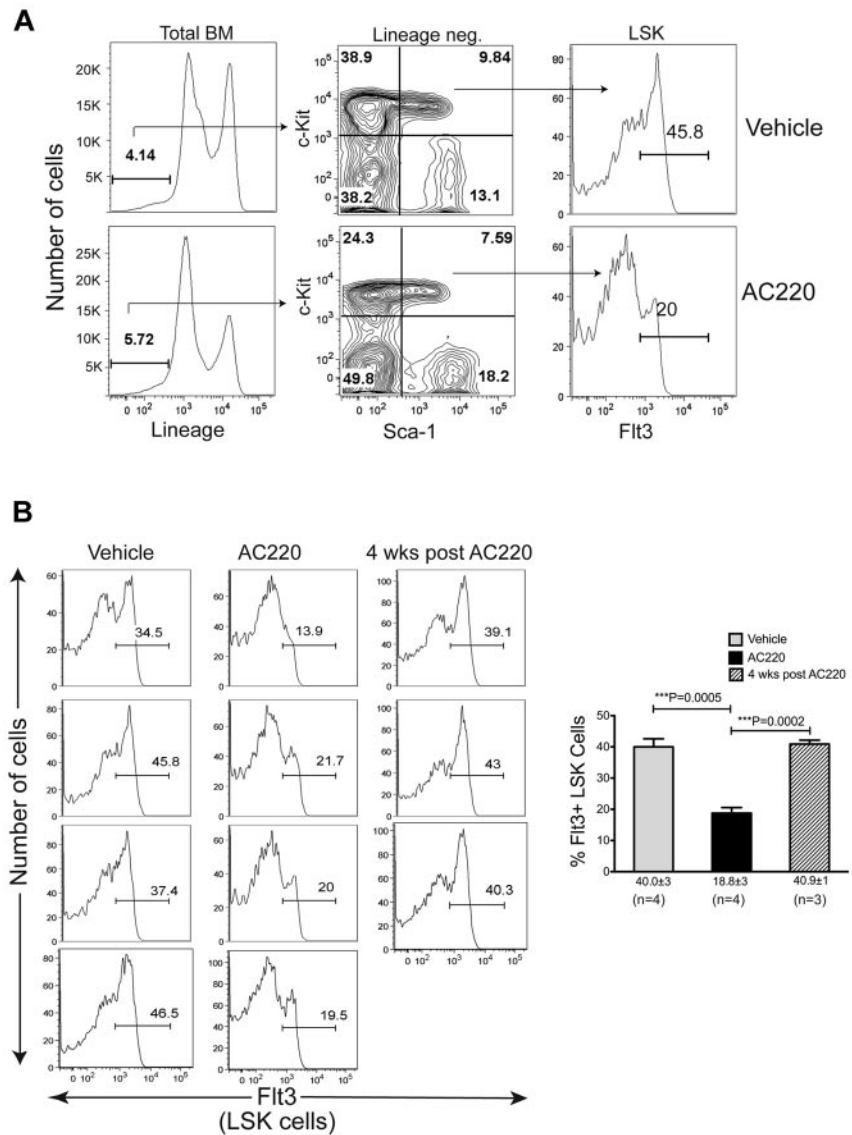
decrease in myeloid cell invasiveness into the liver and lungs compared with their vehicle-treated controls (Figure 3D). These observations suggest that ongoing AC220 treatment has the potential to markedly improve the health and survival of c-Cbl^{A/-} mice. The mice were not dosed for longer periods because of logistics associated with long-term dosing and time restrictions from our institutional ethics committee.

AC220 treatment causes a significant reduction in Flt3⁺ MPPs

One profound effect of the c-Cbl RING finger mutation is the expansion of Flt3⁺ MPPs in the BM, a phenotype not seen in c-Cbl KO mice or Cbl-b RING finger mutant mice.⁴ Furthermore, the expansion of these cells is correlated with disease development, because c-Cbl^{A/-}/Flt3 ligand-knockout double mutant mice show a marked reduction in the number of these cells and do not develop a severe MPD or leukemia.⁴

To determine whether AC220 treatment affects the Flt3⁺ MPP population, we analyzed BM cells isolated from tibias and femurs

Figure 4. Treatment of c-Cbl RING finger mutant mice with AC220 results in a significant reduction in Flt3⁺ MPPs. (A) BM cells were analyzed by flow cytometry and shown are examples of the gating parameters used to identify Lin⁻ cells, LSK cells, and LSK Flt3⁺ cells from c-Cbl^{Δ/Δ} mice treated with vehicle or AC220 for 6 weeks. (B) Cumulative data showing Flt3 profiles of LSK cells from four 8- to 9-month-old c-Cbl^{Δ/Δ} mice that were dosed for 6 weeks with vehicle or AC220. Three mice were also analyzed 4 weeks after AC220 dosing was discontinued. The gate showing the percentage of Flt3⁺ LSK cells is indicated in each profile. The percentages of Flt3⁺ LSK cells for each treatment group are expressed as means ± SEM.



of 4 c-Cbl^{Δ/Δ} mice after 6 weeks of dosing with vehicle or AC220. The total number of nucleated cells was significantly reduced in the AC220-treated mice, resulting in a reduction in the total number of both myeloid and B-lineage cells (supplemental Figure 2A-C). However, the most striking finding from these flow cytometric analyses was the highly significant reduction in Flt3⁺ LSK cells (Figure 4). The specific targeting of Flt3⁺ MPPs is highlighted by the fact that AC220 did not have an equivalent impact on the percentages or numbers of total LSK cells (supplemental Figure 2D-E). When mice were left untreated for 4 weeks after the cessation of AC220 dosing, a reemergence of Flt3⁺ LSK cells was observed (Figure 4B). These results implicate Flt3⁺ progenitors as the key cells that promote MPD development in c-Cbl RING finger mutant mice and suggest that their targeting by AC220 is the mechanism by which the MPD is suppressed.

AC220 rapidly suppresses the proliferative capacity and number of MPPs expressing high levels of Flt3

To investigate the kinetics of AC220-induced suppression of Flt3⁺ MPPs in c-Cbl RING finger mutant mice, we analyzed a cohort of CD45.1^{Δ/Δ} mice over a period of 12 hours to 24 days of daily

dosing with vehicle or AC220. The effects of AC220 on the number and cell-cycle status of MPPs were determined by the expression of the cell-proliferation marker Ki-67. MPPs have been well characterized as a highly proliferative population, with 80%-90% of the cells in cycle as determined by Ki-67 staining.³⁴ Twelve hours after a single dose of AC220, a reduction in the percentage of cells expressing Ki-67 was evident, and this reduction continued through to day 4, when less than 10% of the Flt3⁺ LSK cells expressed Ki-67 (Figure 5B-C). The inhibitory effect of AC220 was also evident by a rapid and significant decrease in cell size (determined by forward light scatter; Figure 5B,D) and by day 4, approximately 90% of the Flt3⁺ cells were small, Ki-67⁻ cells (Figure 5B), a phenotype consistent with quiescence.

Concomitant with the induction of quiescence was a significant reduction in the percentage of Flt3⁺ LSK cells (Figure 5E), and this loss was most notable within the population expressing high levels of Flt3 (Figure 5A). However, the loss of Flt3^{hi} MPPs did not appear to involve death, because there was no significant difference between vehicle- and AC220-treated mice in the proportion of cells undergoing apoptosis (ie, annexin V⁺ propidium iodide⁻ cells; Figure 5F). These findings indicate that the loss of Flt3⁺ cells over

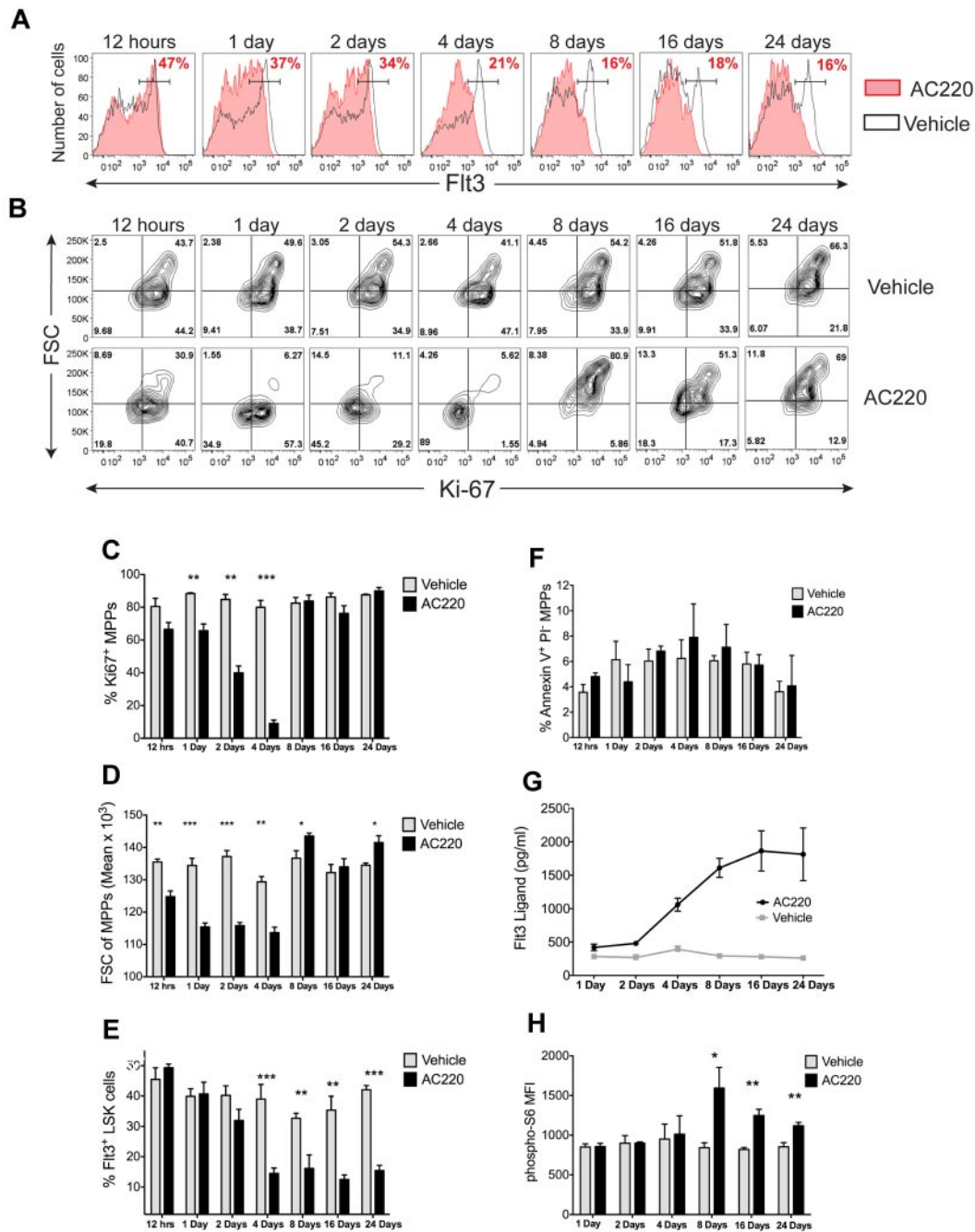


Figure 5. AC220 promotes quiescence and a marked reduction of Flt3⁺ LSK cells, which is followed by a proliferative recovery response that parallels the induction of Flt3 ligand. (A) B6.CD45.1 mice repopulated with c-Cbl^{ΔV} BM were dosed daily with vehicle or 10 mg/kg of AC220, and the BM cells were analyzed by flow cytometry at the indicated time points. The Flt3 profiles are of LSK cells, and the percentages of Flt3⁺ LSK cells (ie, MPPs) from each AC220-treated mouse is shown in red. (B) The gated Flt3⁺ LSK cells in panel A were analyzed for expression of Ki-67 and cell size (forward light scatter, FSC). The percentage of cells in each quadrant is shown. Cells in the top right quadrant are large Ki-67⁺ cells (ie, highly proliferative cells), and the cells in the lower left quadrant are small Ki-67⁻ cells (ie, G₀ quiescent cells). The profiles in panels A and B are representative of 3 vehicle- and 3 AC220-treated mice examined at each of the time points. (C-E) Data from 3 vehicle- and 3 AC220-treated mice examined at each time point showing the percentage of Ki-67⁺ MPPs (C), the geometric mean of forward light scatter (FSC) of MPPs (D), and the percentage of MPPs in the LSK population (E). (F) AC220 shows no effect in promoting apoptosis in MPPs. BM cells were stained with annexin V-FITC and propidium iodide (PI) and gated on the Flt3⁺ LSK population. (G) AC220 dosing promotes the induction of Flt3 ligand. Mice dosed daily with AC220 or vehicle were bled by cardiac puncture at the indicated times and their serum assayed for Flt3 ligand levels by ELISA. The data are from 3-7 mice at each time point. (H) The induction of phospho-S6 in MPPs parallels the increase in Flt3 ligand. The levels of intracellular phospho-S6 in gated Flt3⁺ LSK cells were determined by flow cytometry. The data are from 3 vehicle- and 3 AC220-mice at each time point. Data are means ± SEM. **P* < .05; ***P* < .01; ****P* < .001 using unpaired Student *t* test.

the first 4 days of dosing is due to the ability of AC220 to promote quiescence rather than cytotoxicity. Furthermore, the induction of quiescence in the MPP population did not enhance their differentiation toward common myeloid, megakaryocyte/erythroid, or lymphoid progenitors (supplemental Figure 3A-C).

Flt3⁺ MPPs from AC220-treated mice revert from quiescence to proliferation through a Flt3 ligand-compensatory signal

The quiescence of MPPs observed at day 4 of AC220 dosing was dramatically reversed to a highly proliferative state by day 8, when

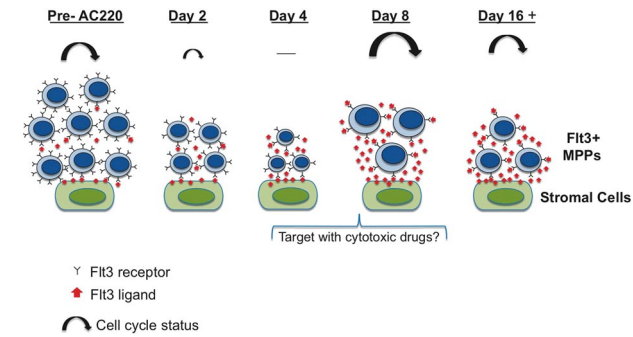


Figure 6. Schematic illustrating the effects of AC220 on MPPs and the FLT3 ligand-associated recovery response. Over the first 4 days of treatment, AC220 promotes quiescence of MPPs, resulting in a marked reduction in their numbers and the expression of FLT3 receptors (illustrated by the small noncycling cells on day 4 with fewer FLT3 receptors). We propose that the loss of MPPs and the reduction of FLT3 expression during these first 4 days are detected by the BM stromal cells, possibly through fewer interactions with membrane-bound FLT3 ligand. This triggers a strong signal that results in the stromal cells markedly increasing their production of FLT3 ligand (red arrows). The resultant robust response by FLT3 ligand then restores the proliferative capacity of the MPPs. From our data shown in Figure 5, it can be seen that the proliferative response on day 8 is even stronger than that seen in c-Cbl RING finger mutant mice that were not treated with AC220 (illustrated by their larger size and the larger cycling arrows). Beyond this point, a steady state is established in which the proliferation driven by high levels of FLT3 ligand is kept in check by the inhibitory effects of AC220, the net effect being that the numbers of MPPs do not increase beyond the initial reduction that occurred during the first 4 days of treatment.

80%-90% of the cells were found to be Ki-67⁺ and slightly larger than cells from vehicle-treated mice (Figure 5B-D). This highly proliferative state was maintained to our end point at day 24 (Figure 5B-C), with similar percentages of MPPs in the G₁ and S + G₂/M phases in the vehicle- and AC220-treated groups at this time (supplemental Figure 4A-B). As a result of this proliferation, the number of FLT3⁺ cells decreased no further and were maintained at the low level reached by day 4 of AC220 dosing (Figure 5E). Therefore, the key inhibitory effect of AC220 is implemented within the first 4 days of dosing, which is followed by a robust recovery response time when small numbers of MPPs return to cycle, but their numbers do not rebound to pretreatment levels as long as AC220 dosing is maintained.

The reversion to proliferation by the MPPs from AC220-treated mice was found to be correlated with the induction of FLT3 ligand, which peaked and plateaued at day 8 to a level 5, which was 6 times higher than vehicle-treated mice (Figure 5G) and remained constant as long as dosing was maintained. This rapid compensatory response to AC220 is most likely mediated via a strong feedback signal that is transmitted by the remaining quiescent FLT3^{lo} cells to FLT3 ligand-expressing stromal cells (shown schematically in Figure 6). However, despite the high levels of FLT3 ligand, AC220 was still capable of maintaining its inhibitory effect because the numbers of MPPs did not increase. Therefore, a delicate balance exists between the inhibitory effects of AC220 and the proliferative signals mediated by the FLT3 receptor/FLT3 ligand interaction. This balance does appear to be preceded by a degree of fine-tuning, because the recovery response was slightly stronger at day 8, as shown by the greater cell size compared with vehicle-treated cells (Figure 5D). This peak in the response is also illustrated by the induction of phospho-S6 at day 8 of AC220 dosing (Figure 5H), a time when the cells are first exposed to high levels of FLT3 ligand (Figure 5G). Phospho-S6 is a downstream target of the PI3K/mTOR pathway and is a well-characterized measure of FLT3 ligand-induced signaling responses in hematopoietic progenitors.^{35,36} Because phospho-S6 is currently being used to monitor the

biochemical efficacy of AC220 in AML patients,³⁷ it was surprising that no decrease in phospho-S6 levels was evident during the first 4 days of AC220 dosing. Therefore, phospho-S6 may not be a useful biomarker of FLT3 inhibition in this system. If the inhibitory effects of AC220 seen by day 4 had persisted and the FLT3 ligand response had not occurred, it is likely that the hematopoietic system would ultimately fail given the critical role of MPPs. The importance and specificity of the FLT3 ligand in promoting this recovery is further underscored by the finding that SCF levels were not significantly affected by AC220 (Figure 7A). Further, FLT3 ligand levels returned to normal within 12 days of AC220 dosing being discontinued (Figure 7B).

Discussion

In the present study, we show that AC220 was a very effective treatment in a mouse model of MPD driven by wild-type FLT3. The c-Cbl RING finger mutant mouse develops a severe MPD that exhibits enhanced FLT3 signaling and an expanded population of MPPs expressing high levels of FLT3.⁴ By targeting these progenitors in the BM, AC220 markedly reduces their numbers and also

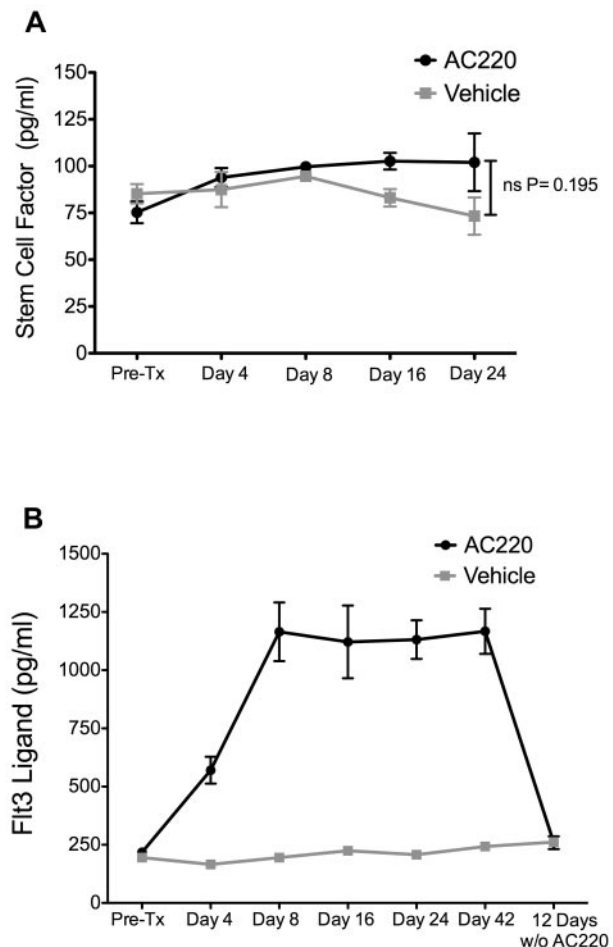


Figure 7. SCF levels are not significantly affected by AC220 dosing and FLT3 ligand levels return to normal within 12 days after AC220 dosing is discontinued. Eight-month-old c-Cbl^{fl/fl} mice were dosed daily with AC220 or vehicle and bled from the tail vein at the indicated times. In the experiment shown in panel B, mice were dosed daily for 42 days and then left untreated for 12 days. The levels of (A) SCF and (B) FLT3 ligand were measured by ELISA. Four vehicle- and 4 AC220-treated c-Cbl^{fl/fl} mice were followed for the length of the experiment. Serum levels (pg/mL) are shown as means ± SEM.

the levels of Flt3 expression, resulting in a reversion of the MPD. To the best of our knowledge this study is the first to demonstrate the effectiveness of an Flt3 kinase inhibitor for treating a disease or disorder associated with enhanced wild-type Flt3 signaling.

The concept of targeting wild-type Flt3 for treating hematopoietic neoplasms is not novel,^{2,38} but previous attempts were hindered by Flt3 inhibitors with inadequate specificity, potency, and pharmacokinetic properties. We have shown herein that the second-generation Flt3 inhibitor AC220 overcomes these inadequacies, suggesting that its use could be broadened to treat a range of leukemias characterized by high levels of Flt3 expression (eg, in mixed-lineage leukemias).³⁹⁻⁴¹ Indeed, the Flt3 inhibitor lestauritinib is currently being examined as a treatment for mixed-lineage leukemias in a group-wide phase 3 study from the Children's Oncology Group. However results from clinical trials with lestauritinib have been disappointing because of suboptimal activity in plasma⁴² and inadequate kinase specificity.³⁰ For these reasons, and because of the effects seen in the present study, AC220 offers greater promise as a treatment for leukemias associated with enhanced wild-type Flt3 signaling.

Key findings from the present study came from analyzing the early effects of AC220 in its promotion of quiescence of the targeted progenitor population, which was followed by a rapid proliferative recovery that paralleled the induction of Flt3 ligand. It has recently become apparent that the induction of Flt3 ligand impedes the efficacy of Flt3 inhibitors,⁴³ and understanding how this affects their potency and how this can be best managed is of significance for many leukemia patients. We show herein that AC220 is clearly at its most potent over the first 4 days of treatment by inducing quiescence in > 90% of the MPPs (Figure 5C), causing a marked reduction in their numbers (Figure 5E). However, this potency is blunted and the downward trend in MPP numbers halted by a robust Flt3 ligand-induced recovery that occurs by day 8 (Figure 5G). Therefore, the counterbalance mediated by the Flt3 ligand provides an opposing force to AC220, creating a stable environment that allows the Flt3⁺ progenitors to cycle at a rate that is remarkably similar to that of vehicle-treated mice (Figure 5C and supplemental Figure 3D-E). Once the numbers of Flt3⁺ cells have been reduced over the first 4 days of dosing, the combination of AC220 and Flt3 ligand maintain a constant but low level of Flt3⁺ cells, and this level is sufficient to suppress MPD development.

Our observations on the action of AC220 suggest that the efficacy of treatment might be improved with compounds that target the production of Flt3 ligand (which, in the BM, is from stromal fibroblasts) or by the administration of Flt3 ligand Abs or antagonists, which could disrupt this delicate balance and provide more effective treatments for leukemias dependent on Flt3 signaling. Furthermore, the rapid reversion from quiescence to proliferation by the AC220-targeted cells between days 4 and 8 (Figure 5C) may offer a window of opportunity in which these cells are likely to be highly susceptible to cytotoxic drugs (Figure 6). Monitoring patient serum levels for Flt3 ligand production over the first few weeks of Flt3 inhibitor treatment could provide predictive data for the most appropriate time to introduce cytotoxic drugs.

In summary, the results of the present study have shown that a mouse model of MPD driven by wild-type Flt3 can be effectively

treated with a potent and highly selective Flt3 inhibitor, indicating that patients with c-Cbl mutations, and those with similarly enhanced wild-type Flt3 signaling, may respond well to AC220. Indeed, our data indicate that AC220 may induce remission in patients with c-Cbl mutations and, therefore, may allow these patients time to recover sufficient strength for stem cell transplantation. This study also demonstrates that AC220 mediates its key effects over the first 4 days, after which a robust Flt3 ligand-mediated recovery response is triggered, creating a delicate balance between these opposing forces. Monitoring Flt3 ligand production in clinical studies may provide an indication of a patient's response to Flt3 inhibitors and guide the timing for administering cytotoxic drugs. Furthermore, our findings suggest that future studies aimed at identifying the signaling events that trigger the induction of Flt3 ligand could lead to the development of novel compounds that would allow Flt3 inhibitors to work with greater potency and for extended periods.

Acknowledgments

The authors thank Drs Patrick Zarrinkar, Mohit Trikha, and David O'Neill from Ambit Biosciences for supplying AC220 (quizartinib); Ms Karen Waldock from the Sir Charles Gairdner Hospital Cancer Center for mouse irradiation; Ms Slavica Pervan for preparing the histopathology sections; Mr Rey Robayna for help with preparation of figures; and the Australian Microscopy & Microanalysis Research Facility at the Center for Microscopy, Characterization & Analysis, The University of Western Australia (a facility funded by the University, State and Commonwealth Government) for the use of facilities and for scientific and technical assistance.

This work was supported by the National Health and Medical Research Council (project grants 572516 and 634414) and by the Medical and Health Research Infrastructure Fund (Health Department of Western Australia).

Authorship

Contribution: S.J.T. designed, performed, and analyzed the data for the experiments summarized in Figures 5 and 7 and supplemental Figures 3 and 4; S.A.D. established the cohorts of transplanted mice and contributed to the dosing and bleeding of mice; C.B.F.T. established the initial c-Cbl^{Δ/Δ} cohort, prepared the images in Figure 3, and helped edit the manuscript; M.E.W. provided help and advice on the running and analyzing of cells for flow cytometry and with editing the manuscript; and W.Y.L. conceived the study, carried out the experiments summarized in Figures 1 through 4 and supplemental Figures 1 and 2, analyzed the data, and wrote the manuscript.

Conflict-of-interest disclosure: The authors declare no competing financial interests.

Correspondence: Wallace Y. Langdon, PhD, School of Pathology and Laboratory Medicine, University of Western Australia, 35 Stirling Highway, Crawley, Western Australia, 6009 Australia; e-mail: wally.langdon@uwa.edu.au.

References

- Gilliland DG, Griffin JD. The roles of FLT3 in hematopoiesis and leukemia. *Blood*. 2002;100(5):1532-1542.
- Armstrong SA, Kung AL, Mabon ME, et al. Inhibition of FLT3 in MLL. Validation of a therapeutic target identified by gene expression based classification. *Cancer Cell*. 2003;3(2):173-183.
- Zheng R, Levis M, Piloto O, et al. FLT3 ligand causes autocrine signaling in acute myeloid leukemia cells. *Blood*. 2004;103(1):267-274.
- Rathinam C, Thien CBF, Flavell RA, Langdon WY. Myeloid Leukemia Development in c-Cbl RING

- Finger Mutant Mice is Dependent on FLT3 Signaling. *Cancer Cell*. 2010;18(4):341-352.
5. Lai AY, Kondo M. Asymmetrical lymphoid and myeloid lineage commitment in multipotent hematopoietic progenitors. *J Exp Med*. 2006;203(8):1867-1873.
 6. Dunbar AJ, Gondek LP, O'Keefe CL, et al. 250K single nucleotide polymorphism array karyotyping identifies acquired uniparental disomy and homozygous mutations, including novel missense substitutions of c-Cbl in myeloid malignancies. *Cancer Res*. 2008;68(24):10349-10357.
 7. Makishima H, Cazzolli H, Szpurka H, et al. Mutations of E3 ubiquitin ligase Cbl family members constitute a novel common pathogenic lesion in myeloid malignancies. *J Clin Oncol*. 2009;27(36):6109-6116.
 8. Grand F, Hidalgo-Curtis C, Ernst T, et al. Frequent Cbl mutations associated with 11q acquired uniparental disomy in myeloproliferative neoplasms. *Blood*. 2009;113:6182-6192.
 9. Loh ML, Sakai DS, Flotho C, et al. Mutations in CBL occur frequently in juvenile myelomonocytic leukemia. *Blood*. 2009;114(9):1859-1863.
 10. Muramatsu H, Makishima H, Jankowska AM, et al. Mutations of an E3 ubiquitin ligase c-Cbl but not TET2 mutations are pathogenic in juvenile myelomonocytic leukemia. *Blood*. 2010;115(10):1969-1975.
 11. Kohlmann A, Grossmann V, Klein HU, et al. Next-generation sequencing technology reveals a characteristic pattern of molecular mutations in 72.8% of chronic myelomonocytic leukemia by detecting frequent alterations in TET2, CBL, RAS, and RUNX1. *J Clin Oncol*. 2010;28(24):3858-3865.
 12. Sanada M, Suzuki T, Shih L-Y, et al. Gain-of-function of mutated C-CBL tumour suppressor in myeloid neoplasms. *Nature*. 2009;460(7257):904-908.
 13. Schnittger S, Bacher U, Eder C, et al. Molecular analyses of 15,542 patients with suspected BCR-ABL1-negative myeloproliferative disorders allow to develop a stepwise diagnostic workflow [published online ahead of print April 17, 2012]. *Haematologica*. doi:10.3324/haematol.2012.064683.
 14. Schnittger S, Bacher U, Alpermann T, et al. Use of CBL exon 8 and 9 mutations in diagnosis of myeloproliferative neoplasms and myeloproliferative/myelodysplastic disorders: an analysis of 636 cases [published online ahead of print June 24, 2012]. *Haematologica*. doi:10.3324/haematol.2012.065375.
 15. Onida F, Kantarjian HM, Smith TL, et al. Prognostic factors and scoring systems in chronic myelomonocytic leukemia: a retrospective analysis of 213 patients. *Blood*. 2002;99(3):840-849.
 16. Ma X, Does M, Raza A, Mayne ST. Myelodysplastic syndromes incidence and survival in the United States. *Cancer*. 2007;109(8):1536-1542.
 17. Kao HW, Sanada M, Liang DC, et al. A high occurrence of acquisition and/or expansion of C-CBL mutant clones in the progression of high-risk myelodysplastic syndrome to acute myeloid leukemia. *Neoplasia*. 2011;13(11):1035-1042.
 18. Sargin B, Choudhary C, Crosetto N, et al. FLT3-dependent transformation by inactivating c-Cbl mutations. *Blood*. 2007;110(3):1004-1012.
 19. Caligiuri MA, Briesewitz R, Yu J, et al. Novel c-Cbl and Cbl-b ubiquitin ligase mutations in human acute myeloid leukemia. *Blood*. 2007;110(3):1022-1024.
 20. Abbas S, Rotmans G, Lowenberg B, Valk PJM. Exon 8 splice site mutations in the gene encoding the E3-ligase CBL are associated with core binding factor acute myeloid leukemias. *Haematologica*. 2008;93(10):1595-1597.
 21. Reindl C, Quentmeier H, Petropoulos K, et al. CBL exon8/9 mutants activate the FLT3 pathway and cluster in core binding factor/11q deletion acute myeloid leukemia/myelodysplastic syndrome subtypes. *Clin Cancer Res*. 2009;15(7):2238-2247.
 22. Fernandes MS, Reddy MM, Croteau NJ, et al. Novel oncogenic mutations of CBL in human acute myeloid leukemia that activate growth and survival pathways depend on increased metabolism. *J Biol Chem*. 2010;285(42):32596-32605.
 23. Makishima H, Jankowska AM, McDevitt MA, et al. CBL, CBLB, TET2, ASXL1, and IDH1/2 mutations and additional chromosomal aberrations constitute molecular events in chronic myelogenous leukemia. *Blood*. 2011;117(21):e198-e206.
 24. Nicholson L, Knight T, Matheson E, et al. Casitas B lymphoma mutations in childhood acute lymphoblastic leukemia. *Genes Chrom Cancer*. 2012;51(3):250-256.
 25. Shiba N, Park MJ, Taki T, et al. CBL mutations in infant acute lymphoblastic leukaemia. *Br J Haematol*. 2012;156(5):672-674.
 26. Shiba N, Taki T, Park MJ, et al. CBL mutation in childhood therapy-related leukemia. *Leukemia*. 2011;25(8):1356-1358.
 27. Levkowitz G, Waterman H, Ettenberg SA, et al. Ubiquitin ligase activity and tyrosine phosphorylation underlie suppression of growth factor signaling by c-Cbl/Sli-1. *Mol Cell*. 1999;4(6):1029-1040.
 28. Thien CBF, Walker F, Langdon WY. Ring finger mutations that abolish c-Cbl-directed polyubiquitination and downregulation of the EGF receptor are insufficient for cell transformation. *Mol Cell*. 2001;7(2):355-365.
 29. Joazeiro CAP, Wing SS, Huang H-K, Levenson JD, Hunter T, Liu Y-C. The tyrosine kinase negative regulator c-Cbl as a RING-type, E2-dependent ubiquitin-protein ligase. *Science*. 1999;286:309-312.
 30. Zarrinkar PP, Gunawardane RN, Cramer MD, et al. AC220 is a uniquely potent selective inhibitor of FLT3 for the treatment of acute myeloid leukemia (AML). *Blood*. 2009;114(14):2984-2992.
 31. Cortes JE, Perl AE, Smith CC, et al. A phase II open-label, AC220 monotherapy efficacy study in patients with refractory/relapsed FLT3-ITD positive acute myeloid leukemia: updated interim results [abstract]. *Blood (ASH Annual Meeting Abstracts)*. 2011;118(21):2576.
 32. Thien CBF, Blystad FD, Zhan Y, et al. Loss of c-Cbl RING finger function results in high-intensity signaling and thymic deletion. *EMBO J*. 2005;24(21):3807-3819.
 33. Smith CC, Wang Q, Chin CS, et al. Validation of ITD mutations in FLT3 as a therapeutic target in human acute myeloid leukaemia. *Nature*. 2012;485(7397):260-263.
 34. Wilson A, Laurenti E, Oser G, et al. Hematopoietic stem cells reversibly switch from dormancy to self-renewal during homeostasis and repair. *Cell*. 2008;135(6):1118-1129.
 35. Marvin J, Swaminathan S, Kraker G, Chadburn A, Jacobberger J, Goolsby C. Normal bone marrow signal-transduction profiles: a requisite for enhanced detection of signaling dysregulations in AML. *Blood*. 2011;117(15):e120-e130.
 36. Woost PG, Solchaga LA, Meyerson HJ, Shankey TV, Goolsby CL, Jacobberger JW. High-resolution kinetics of cytokine signaling in human CD34/CD117-positive cells in unfractionated bone marrow. *Blood*. 2011;117(15):e131-e141.
 37. Perl AE, Jeschke GR, Smith CC, Mangan JK, Luger SM, Carroll M. Phospho-specific flow cytometry of fixed whole blood demonstrates in vivo FLT3 inhibition in circulating leukemic blasts during AC220 therapy and accurately detects the development of therapeutic resistance [abstract]. *Blood (ASH Annual Meeting Abstracts)*. 2011;118(21):3502.
 38. Wang CM, Sheng GY, Lu J, et al. Effect of small interfering RNA targeting wild-type FLT3 in acute myeloid leukaemia cells in vitro and in vivo. *J Int Med Res*. 2011;39(5):1661-1674.
 39. Wei J, Wunderlich M, Fox C, et al. Microenvironment determines lineage fate in a human model of MLL-AF9 leukemia. *Cancer Cell*. 2008;13(6):483-495.
 40. Armstrong SA, Staunton JE, Silverman LB, et al. MLL translocations specify a distinct gene expression profile that distinguishes a unique leukemia. *Nat Genet*. 2002;30(1):41-47.
 41. Ferrando AA, Armstrong SA, Neuberg DS, et al. Gene expression signatures in MLL-rearranged T-lineage and B-precursor acute leukemias: dominance of HOX dysregulation. *Blood*. 2003;102(1):262-268.
 42. Pratz KW, Sato T, Murphy KM, Stine A, Rajkhowa T, Lewis M. FLT3-mutant allelic burden and clinical status are predictive of response to FLT3 inhibitors in AML. *Blood*. 2010;115(7):1425-1432.
 43. Sato T, Yang X, Knapper S, et al. FLT3 ligand impedes the efficacy of FLT3 inhibitors in vitro and in vivo. *Blood*. 2011;117(12):3286-3293.